



International Conference and Workshop on Chemical Engineering UNPAR 2013, ICCE UNPAR 2013

The characteristics of green calcium oxide derived from aquatic materials

Soipatta Soisuwan^{a,*}, Jiraporn Phommachant^a, Wilasinee Wisaijorn^a,
Piyasan Prasertdam^b

^aDepartment of Chemical Engineering, Faculty of Engineering, Burapha University, 169 Long-Hard Bangsaen Road, Saensuk Sub-district, Muang District, Chonburi, 20131, Thailand

^bCenter of Excellence in Catalysis and Catalytic Reaction Engineering, Department of Chemical Engineering, Faculty of Engineering, Chulalongkorn University, Patumwan District, Bangkok, 10330, Thailand

Abstract

Thermogravimetric Analysis of three aquatic materials, i.e. cuttlebone, mussel shell and oyster shell, and other physicochemical characteristics were investigated. The highest decomposition rates of aquatic materials under two surrounding gases, i.e. oxygen and nitrogen, exhibited no significant difference for cuttlebone (3.6×10^{-5} – 4.8×10^{-5} $\text{mg s}^{-1} \text{mg}_{\text{initial}}^{-1}$ at heating rate $5^\circ\text{C}/\text{min}$ and 11.8×10^{-5} – 12.5×10^{-5} $\text{mg s}^{-1} \text{mg}_{\text{initial}}^{-1}$ at heating rate $15^\circ\text{C}/\text{min}$) and mussel shell (3.4×10^{-5} – 5.2×10^{-5} $\text{mg s}^{-1} \text{mg}_{\text{initial}}^{-1}$ at heating rate $5^\circ\text{C}/\text{min}$ and 11.9×10^{-5} – 12.4×10^{-5} $\text{mg s}^{-1} \text{mg}_{\text{initial}}^{-1}$ at heating rate $15^\circ\text{C}/\text{min}$), while oyster shell provided the higher decomposition rate under nitrogen surrounding gas (7.6×10^{-4} $\text{mg s}^{-1} \text{mg}_{\text{initial}}^{-1}$ at heat rate $5^\circ\text{C}/\text{min}$ and 21.53×10^{-4} $\text{mg s}^{-1} \text{mg}_{\text{initial}}^{-1}$ at heating rate $15^\circ\text{C}/\text{min}$). This is probably because of the difference in their starting crystalline structures, i.e. aragonite (cuttlebone and mussel shell) and calcite (oyster shell). The cubic calcium oxides were prepared by calcination of three aquatic materials under oxygen and nitrogen surrounding gases at $5^\circ\text{C}/\text{min}$ ramping to 850°C for 2 hours. All resulting calcium oxides obtained from oxygen atmosphere provided only cubic crystalline phases and the adsorption-desorption isotherms (IUPAC Type III), whereas the calcinations under nitrogen surrounding gas gave a presence of calcium hydroxide crystalline or hydroxyl-contaminate existing with cubic calcium oxide that influences on the strength and the number of carbon dioxide adsorption sites. The specific surface area of all resulting calcium oxides ranged from $0.1 - 1.5 \text{ m}^2/\text{g}$ and the average pore diameter was found in the range of 40–60 nm. The the number of basic sites belonging to CaO derived from Oyster shell or Cuttlebone were improved while firing under oxygen atmosphere. The suitable firing condition is at the low heating rate to develop porous materials.

* Corresponding author. Tel.: +6-638-102-222 ext. 335 ; fax: +6-638-745-806
E-mail address: soipatta@buu.ac.th

© 2014 The Authors. Published by Elsevier B.V. This is an open access article under the CC BY-NC-ND license (<http://creativecommons.org/licenses/by-nc-nd/3.0/>).

Peer-review under responsibility of the Organizing Committee of ICCE UNPAR 2013

Keywords: aquatic material; calcium oxide; calcination; and physicochemical property

1. Introduction

Aquatic material is one of interesting materials which consists of high content of calcium carbonate. The materials can endothermically decompose to deliberate carbon dioxide and provide calcium oxide which is more valuable material. The applications of calcium oxide are versatile such as production of mortar for constructions, reinforcing filler in polymer materials¹, reconstruction of bone defect as bone filler², sorbent for CO₂ capture^{3,4}. Besides that, calcium oxide has been recently used as catalytic materials. As calcium oxide possesses high amount of base sites, the potentials to exploit it as the catalyst is great and it has been recently used as solid catalyst for biodiesel productions⁵. The alkali-doped calcium oxide catalysts were active for oxidative coupling of methane⁶ and it was used as a catalyst promotor for several reactions. The calcium oxide promoted Ni catalyst supported on tetragonal zirconia improved the reaction of dry reforming⁷. The natural calcium sources are available abundantly in ecosystem, generally existing in term of calcium carbonate. A common process that converts natural calcium sources to calcium oxide is high-temperature-firing. The process can deliberate structural carbons as carbon dioxide molecules and calcium oxide remains as residue. The applications of calcium oxide are versatile, especially in catalysis because of basic surface properties which are significant to several reaction mechanisms such as dehydration esterification and transesterification etc. The natural aquatic materials, i.e. cuttlebone, mussel shell and oyster shell were introduced as calcium sources in our experiment. The kinetics of calcium carbonate decomposition for these materials under two different surrounding gases i.e. oxygen and nitrogen were investigated at various heating rate (5, 10 and 15 °C/min). The physical properties of natural raw materials and derived calcium oxide were characterized by Scanning Electron Microscopy and Energy Dispersive X-ray Spectroscopy (SEM-EDXS), X-ray diffraction (XRD), N₂ physisorption and CO₂ Temperature Programmed-Desorption (CO₂-TPD).

2. Experiment

2.1. Material Preparation

Three aquatic materials i.e. cuttlebone, mussel shell and oyster shell were chosen as representative materials to investigate thermal decomposition by Thermogravimetric Analysis (TGA) and their characteristics after calcinations. The clean aquatic materials were ground to fine particles. Thermal –Gravimetric Analysis (Mettler Toledo, TGA850) was carried out under dynamics oxygen or nitrogen atmosphere (25 ml/min) at three different heating rates (5, 10 and 15 °C/min) in order to determine their decomposition rates and temperatures of the highest decomposition. The grinded materials were calcined at 850 °C in order to obtain the resulting powder under oxygen or nitrogen atmosphere with heating rate 5 °C/min for 2 hours. The resulting powders were characterized by means of N₂ physisorption, X-ray Diffraction (XRD), Scanning Electron Microscope (SEM) and Energy Dispersive X-ray Spectroscopy (EDXS), and CO₂ Temperature Programmed Desorption (CO₂-TPD).

2.2. Material Characterizations

All resulting materials were characterized by means of X-ray Diffraction, N₂ physisorption, Scanning Electron Microscope (SEM) and Energy Dispersive X-ray Spectroscopy (EDXS). X-ray diffraction (XRD) was examined by SEIMENS D5000 with using CuK_α and Ni filter. Prior to N₂ physisorption, sample was degassed at 300 °C in order to physically desorbed gasses existing on sample surface. The N₂ physical adsorption and desorption were carried out at P/P₀ ranging from 0.05 to 0.99 under 77 K and vice versa. The physisorption and desorption were analyzed by Quanta Chrome machine (NOVA 1200). The morphology of raw materials and resulting samples were investigated by Scanning Electron Microscope (SEM) with 2000x magnification and dispersive atomic elements were identified

by Energy Dispersive X-ray Spectroscopy (EDXS). Prior to CO₂ Temperature Programmed Desorption of all synthesized CaO samples, the sample surface was cleaned under N₂ flowing gas at 100 °C and it was fully saturated under CO₂ flowing gas for 6 hours. The CO₂ Temperature Programmed Desorption of all samples was carried out at the heating rate of 10 °C/min ramping from 30 to 800 °C. The amounts of desorbed CO₂ corresponding to desorption areas under CO₂ Temperature Programmed Desorption profiles were reported.

3. Results and discussions

3.1 Thermal Analysis of Raw Materials

The decompositions of raw materials i.e. cuttlebone, mussel shell and oyster shell were investigated under two surrounding gases i.e. nitrogen and oxygen. The thermal decomposition of commercial CaCO₃ was investigated as reference. The temperature was ramped to 1000 °C with 5 °C/min, 10 °C/min and 15 °C/min. All samples gave the weight loss in the range of 40-50% and the thermal decomposition appeared to have been starting obviously at 550 °C and they were likely to end absolutely around 850 °C as shown in Fig. 1 (as same as thermal decomposition of mussel shell and cuttlebone-not shown). The thermal decomposition results under two surrounding gasses were not significantly different (shown only surrounding oxygen gas), but the rates of decomposition calculated by Equation 1 exhibited significant differences for all samples at various heating rates in Fig. 2. The highest decomposition rate of oyster shell were found at 7.6×10^{-4} , 17.07×10^{-4} and 21.53×10^{-4} mg s⁻¹ mg starting material⁻¹ at 5, 10 and 15 °C/min under surrounding nitrogen gas, whereas these heating rates exhibited the highest decomposition rates at 3.2×10^{-5} , 7.3×10^{-5} and 9.8×10^{-5} under surrounding oxygen gas. The highest decomposition rate is the highest rate of weight loss that was derived from the steepest line of weight and time during calcination under the temperature range of 30 to 1000 °C as shown in equation 1.

$$\text{Decomposition rate} = \frac{dw}{dt} \times \frac{1}{\text{initial weight}} \quad (1)$$

where dw/dt was the derivative of weight with respect to time (mg s⁻¹), and the initial weight was the starting weight of raw material. The highest decomposition rates and the highest decomposition temperature increased while the heating rates were changed from 5 °C/min to 15 °C/min for all types of raw materials as shown in Fig.2. This is because the reaction of decomposition is endothermic reaction as shown in equation 4. The rate constant (k) is apparently dependent on the increase of temperature subsequently leading to the higher rate of reaction/decomposition apparently related to the Arrhenius expression (equation 2) and the rate law (equation 3)⁹.

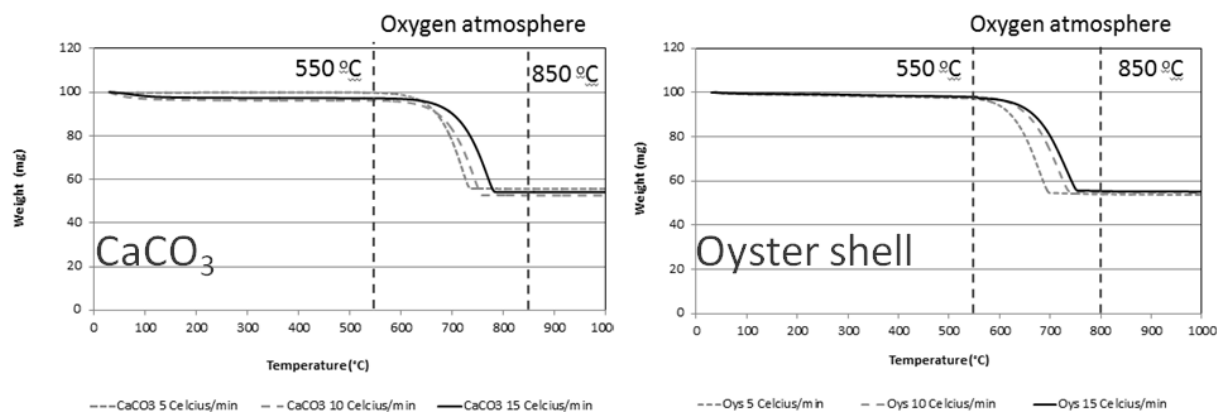


Figure 1 Thermal Gravimetric Analysis of commercial CaCO₃ and oyster shell at 5 °C/min, 10 °C/min and 15 °C/min under oxygen surrounding gas.

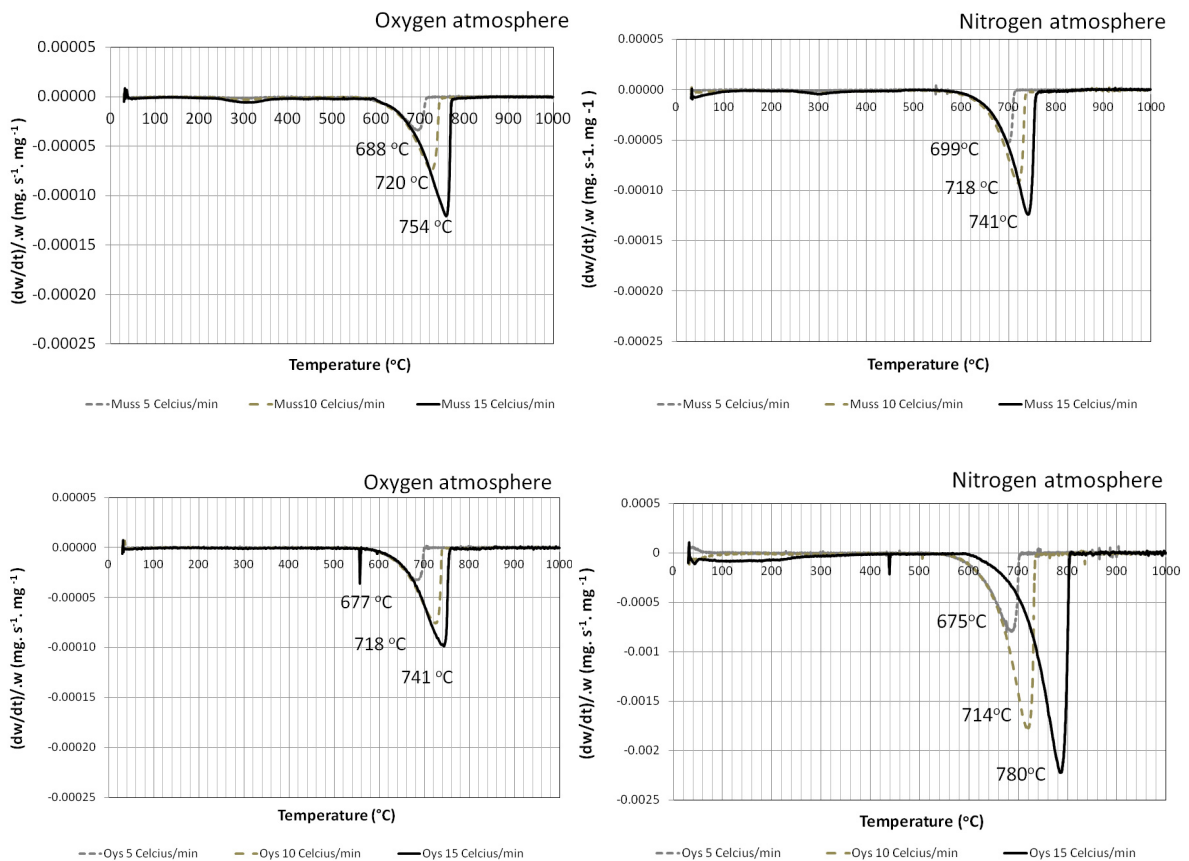
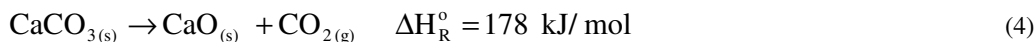


Figure 2 The highest decomposition rates and the highest decomposition temperature of 3 types of raw materials, i.e. cuttlebone (not shown), mussel shell (Fig. 2 upper) and oyster shell (Fig. 2 lower)

$$k = Ae^{-E_a/RT} \quad (2)$$

$$\text{Rate of decomposition} = k[\text{CaCO}_3]^n \quad (3)$$

The empirical (Eq.2) expresses the relationship between temperature (K) and rate constant (k , $\text{mol}^{-n} \text{ liter}^n$), where the constant A is referred to Arrhenius preexponential factor and E_a is the activation energy for the reaction. The increase of decomposition rate in the rate law (Eq.3) is related to rate constant in Arrhenius expression (Eq.2), where $[\text{CaCO}_3]$ is the concentration of calcium carbonate (mol liter^{-1}) and n is the reaction order. The higher heating rate of calcination thereby can rapidly increase the temperature causing higher decomposition temperature and higher decomposition rate as the results shown in Fig.1 and Fig. 2. The comparison of surrounding gasses revealed that the highest decomposition rates under nitrogen atmosphere were found to be higher than those of surrounding oxygen gas in the particular case of oyster shell, whereas cuttlebone and mussel shell exhibited the highest decomposition rates evenly in both surrounding gases. The endothermic decomposition liberates carbon dioxide gas and leave calcium residue as the below equation 4.



There are several factors affecting decomposition of calcium carbonate e.g. composition of raw materials, surrounding gas, carbondioxide concentration etc, whereas the liberation of carbondioxide apparently depend on some factors i.e. i) ability of molecular carbondioxide diffusion into surrounding gas film or an external diffusion and ii) ability of internal carbondioxide diffusion into internal pore of material or an internal diffusion. The carbondioxide diffusion in nitrogen seems to be more active rather than the case of oxygen atmosphere possibly leading to higher decomposition rate in the case of oyster shell, while cuttlebone and mussel shell may not be possible. Structure of raw materials is likely to have an influence on the internal carbon dioxide diffusion in particles. The texture of cuttlebone or mussel shell may not well encourage the internal carbondioxide diffusion which can act as the determining step considerably governing on the rate of decomposition. The step may be plausibly more important than external carbondioxide diffusion in the cases of cuttlebone and mussel shell. The carbondioxide diffusion in both surrounding gases therefore gave no significant difference in the highest decomposition rate as shown in Fig 2.

Table 1. The highest decomposition rates under two different surrounding gases

Raw Materials	The highest decomposition rate ($\text{mg s}^{-1} \text{ mg initial weight}^{-1}$) under two firing gas atmospheres	
	Oxygen surrounding gas	Nitrogen surrounding gas
Cuttlebone		
5	3.6×10^{-5}	4.8×10^{-5}
10	10.2×10^{-5}	7.6×10^{-5}
15	12.5×10^{-5}	11.8×10^{-5}
Mussel shell		
5	3.4×10^{-5}	5.2×10^{-5}
10	7.2×10^{-5}	9.3×10^{-5}
15	11.9×10^{-5}	12.4×10^{-5}
Oyster shell		
5	3.2×10^{-5}	7.60×10^{-4}
10	7.3×10^{-5}	17.07×10^{-4}
15	9.8×10^{-5}	21.53×10^{-4}

3.1 Morphology of raw materials and samples

Scanning Electron Microscope was used to determine the difference in morphology of raw materials and resulting sample in order to clearly identify the conditions of calcination on three types of raw materials, prior to testing their physicochemical properties, i.e. N_2 physisorption and X-ray diffraction. The micrograph shows in Fig. 3 at 3000x magnification. The dense textures of cuttlebone and mussel shell exhibit in Fig. 3 more obviously in comparison with slightly loose texture of oyster shell. These dense textures may not assist the liberation of carbon dioxide during thermal decomposition that can cause the difficulty of internal carbon dioxide diffusion controlling the decomposition rate, subsequently giving no significant change of the highest rate of thermal decomposition under both nitrogen and oxygen surrounding gases. The Energy Dispersive X-ray Spectroscopy identified elements dispersion in raw materials as shown in Table 2. The texture of resulting materials that were calcined at two heating rates i.e. 5 and 15 °C/min as illustrated in Fig. 4 (2000x magnification). The calcinations ramped to 850 °C for 2 hours to obtain resulting powders revealed the sintering at higher heating rate 15 °C/min. The higher heating rate can cause the larger range of particle size distribution leading to decrease in surface area as reported by G.D. Elzinga et al.⁷ Consequently, the heating rate at 5 °C/min and calcination temperature at 850 °C was chosen to prepare the resulting materials for properties characterization.

Table 2 The elements dispersion in raw materials by SEM-EDXS

Raw Materials	% weight of element dispersion in raw materials by EDXS									
	C	O	Na	Mg	Al	Sr	Pb	Ca	Fe	Cl
Cuttlebone	3.68	34.27	2.28	1.29	1.56	4.05	18.98	33.15	0.74	0.00
Mussel Shell	3.23	20.75	4.29	3.00	2.74	7.71	29.43	27.55	1.33	0.00
Oyster Shell	2.72	25.39	2.70	2.17	1.66	4.06	31.15	28.15	0.78	1.25

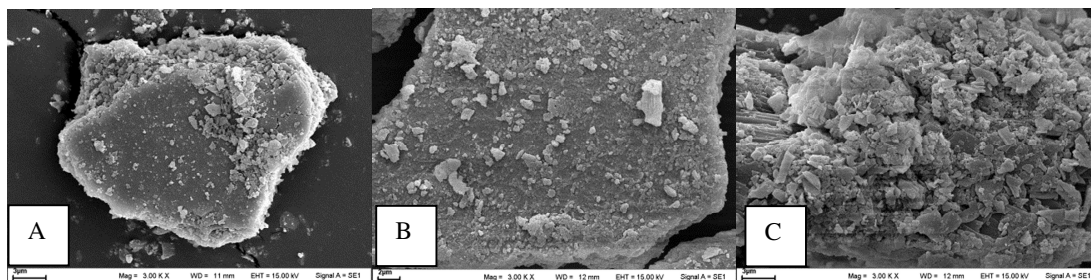


Figure 3 Morphology of raw materials at 3000x magnification (A) cuttlebone, (B) mussel shell and (C) oyster shell

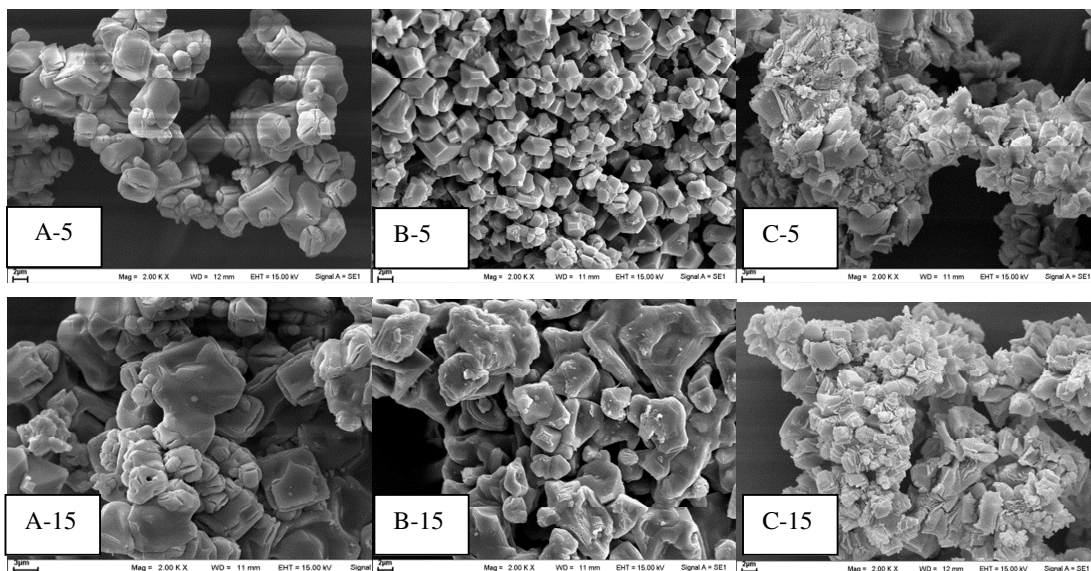


Figure 4 Morphology of resulting materials calcined at various heating rate i.e. (A-5), (A-15) cuttlebone, (B-5), (B-15) mussel shell and (C-5), (C-15) oyster shell at 5 and 15 °C/min

3.2 Characteristics of calcined materials

The X-ray diffraction patterns illustrate in Fig. 5 (A), (B) and (C) for the fresh materials and the resulting sample calcined under oxygen and nitrogen surrounding gases, respectively. All fresh materials composed of crystalline calcium carbonate. The X-ray diffraction pattern revealed calcite structure with hexagonal-rhombohedral shape of oyster shell⁸, while the aragonite structure was found in fresh cuttlebone and mussel shell which was an orthorhombic shape¹. The decomposition of raw materials under oxygen surrounding gas gave clean cubic calcium oxide; on the contrary all resulting materials calcined under nitrogen atmosphere containing cubic calcium oxide structure exhibited small peaks of contaminate calcium hydroxide at $2\theta = 18^\circ, 29.5^\circ, 34^\circ, 47.5^\circ$ and 55° , respectively. The N_2 adsorption and desorption isotherms of all resulting materials are the IUPAC isotherm Type III¹⁰, which an increase of isotherm occurs at high relative P/P_0 , indicating weak adsorbate-adsorbant interactions. The surface areas of all samples were found in the range of 0.15 to 1.3 m^2/g approximately even to commercial cubic calcium oxide which possesses $1.4 \pm 0.3 m^2/g$ (Loba Chemie Pvt. Ltd. (India)). The average pore diameters of all resulting materials are distributed in the range of 44–59 nm. The CO_2 Temperature Programmed Desorption profiles for all derived calcium oxide exhibit in Fig. 6. The strength of carbon dioxide adsorption sites and the number of carbon dioxide adsorption sites are different between all resulting materials fired under different surrounding gases as shown in Table 3. The amount of carbon dioxide desorption can refer to the number of basic sites absorbing acid probe molecules as carbon dioxide. The number of basic sites was based on desorption area of CO_2 temperature programmed profiles. The calcium oxide derived from oyster shell under oxygen atmosphere possesses the highest basic value (16.55×10^4 mole CO_2/g) compared to the others. The calcium oxide prepared under nitrogen atmosphere seems to have higher basic strength because of higher temperature of carbon dioxide desorption. This probably owns to a presence of calcium hydroxide in calcium oxide derived from aquatic materials.

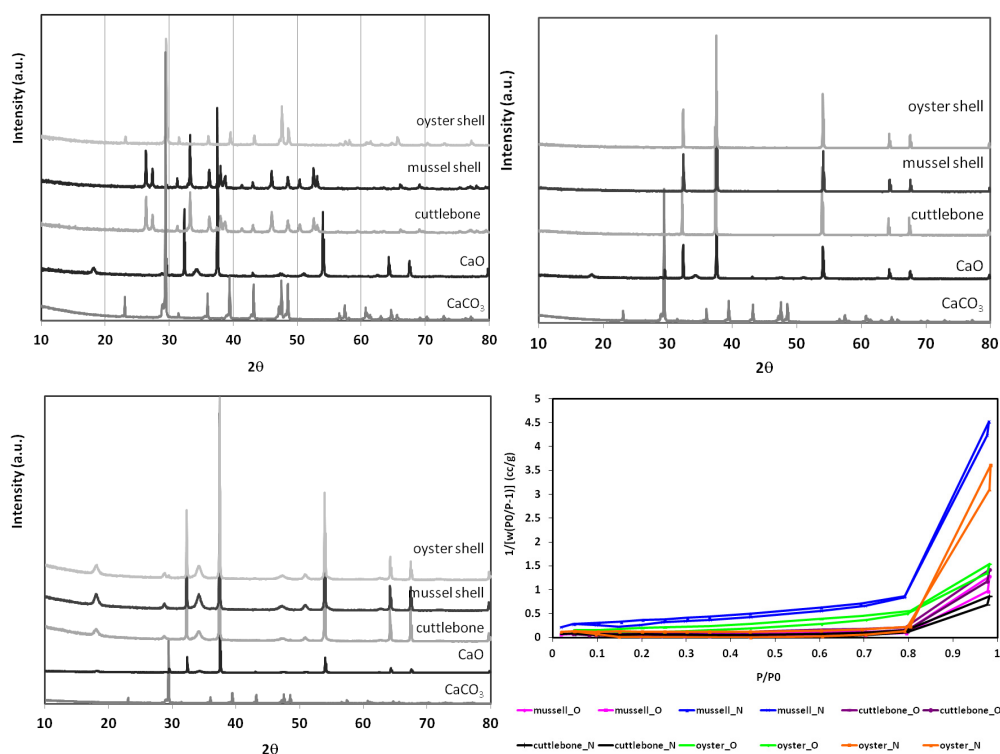


Figure 5 X-ray diffraction patterns of raw materials, resulting materials calcined under two surrounding gases and the isotherms of adsorption-desorption

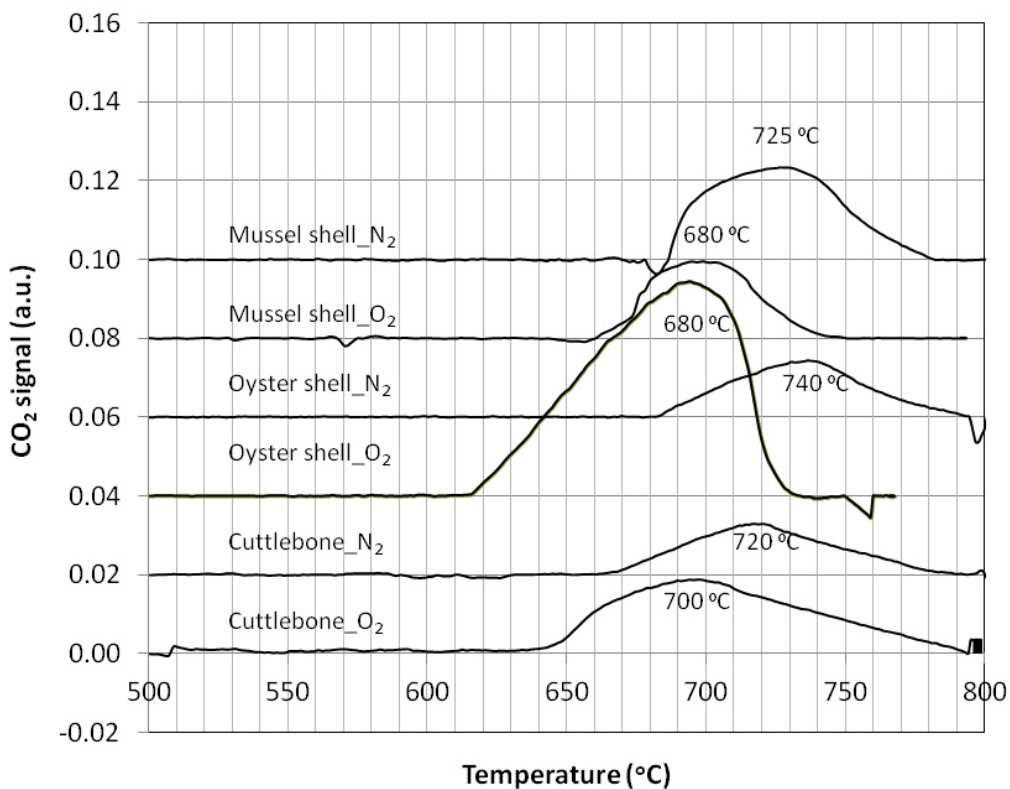


Figure 6 The CO₂ temperature programmed desorption profiles of all derived calcium oxide samples

Table 3 The number of basic sites and desorption temperature of carbondioxide

Sample	The number of basic sites (mole of CO ₂ /g sample) × 10 ⁴	The highest desorption temperature (°C)	BET surface area (m ² /g)	Average pore size diameter (nm)
Cuttlebone_O ₂	7.48	700	0.28	46
Cuttlebone_N ₂	3.76	720	0.14	47
Mussel shell_O ₂	4.14	680	0.25	49
Mussel shell_N ₂	6.38	740	1.24	47
Oyster shell_O ₂	16.55	680	1.38	44
Oyster shell_N ₂	3.81	725	0.32	59

4. Conclusion

The preparation of calcium oxide derived from aquatic materials was suitable at firing temperature 850 °C and heating rate 5 °C/min. The calcinations were carried out under dynamic oxygen or nitrogen atmosphere to obtain cubic calcium oxide. All resulting calcium oxides occurring under oxygen atmosphere provided no significant

difference in crystalline structure and the adsorption-desorption isotherms negligibly regarding to the difference in crystalline structure of starting raw materials. However, calcinations under nitrogen surrounding gas gave a presence of calcium hydroxide crystalline or contaminate existing with cubic calcium oxide that influence on the strength and the number of carbon dioxide adsorption sites. The the number of basic sites belonging to CaO derived from Oyster shell or Cuttlebone were improved while firing under oxygen atmosphere.

5. Acknowledgements

The authors would like to give their gratitude to the Faculty of Engineering, Burapha University for the financial support (Research and Development No. 22/2556), Center of Excellence on Catalysis and Catalytic Reaction Engineering, Chulalongkorn University, Prof. Takanori Miyake, Department of Chemical, Energy and Environmental Engineering, Kansai University, Ms. Tassanee Tubchareon and Ms. Benjamas Netiworaksa.

References

1. Poompradub S, Ikeda Y, Kokubo Y, Shiono T. Cuttlebone as reinforcing filler for natural rubber. *Eur Polym J* 2008; **44**: 4157- 4164
2. Matsuya S, Lin X, Udoh K I, Nakagawa M, Shinmogoryo R, Terada Y, Ishikawa K. Fabrication of porous low crystalline calcite block by carbonation of calcium hydroxide complex. *J Mater Sci-Mater M* 2007; **18**: 1361-7
3. Chen H, Zhao C, Chen M, Li Y, Chen X, CO₂ uptake of modified calcium-based sorbent in a pressurize carbonation-calcination looping. *Fuel Process Technol* 2001; **92**:1144-1151
4. Wei Y L, Lee J H, Formation of priority PAHs from polystyrene pyrolysis with addition of calcium oxide. *Sci Total Environ* 1998; **212**: 173-181
5. Kouzu M, Kasuno T, Tajika M, Yamanaka S, Hidaka J. Active phase calcium oxide use as solid base catalyst for transesterification of soybean oil with refluxing methanol. *Appl Catal A-Gen* 2008; **334**: 357-365
6. Baronetti G T, Padro C, Scelza O A, Castro A A, Cortes Corberan V, Fierro J L G, Structure and reactivity of alkali-doped calcium oxide catalyst for oxidative coupling of methane. *Appl Catal A-Gen* 1993; **101**: 167-183
7. Elzinga G D, Reijers H T J, Cobden P D, Haije W G, van den Brink R W. CaO sorbent stabilisation for CO₂ capture applications. *Energy Procedia* 2011; **4**: 844-851
8. Yadav R R, Mudliar S N, Shekh A Y, Fulke A B, Devi S S, Kishnamurthi K, Juwarkar A, Chakrabarti T. Immobilization of carbonic anhydrase in alginate and its influence on transformation of CO₂ to calcite. *Process Biochem* 2012; **47**: 585-590
9. Engel T, Reid P, *Physical Chemistry*, Pearson Education, Inc., United States, 2010. chapter 35
10. Khafaoui M, Knani S, Hachicha M A, Ben Lamine A. New theoretical expression for the five adsorption type isotherms classified by BET based on statistical physics treatment. *J Colloid Interf Sci*, 2003; **263**: 350-6